doi:10.1111/evo.12743

A new phylogenetic test for comparing multiple high-dimensional evolutionary rates suggests interplay of evolutionary rates and modularity in lanternfishes (Myctophiformes; Myctophidae)

John S. S. Denton[1,2,3] and Dean C. Adams[4]

[1]*Department of Ichthyology and Richard Gilder Graduate School, American Museum of Natural History, New York, New York 10024*

[2]*Current Address: Department of Vertebrate Paleontology, American Museum of Natural History, New York, New York 10024*

[3]*E-mail: jdenton@amnh.org*

[4]*Department of Ecology, Evolution and Organismal Biology, Iowa State University, Ames, Iowa 50011*

Received April 10, 2015
Accepted July 22, 2015

The interplay between evolutionary rates and modularity influences the evolution of organismal body plans by both promoting and constraining the magnitude and direction of trait response to ecological conditions. However, few studies have examined whether the best-fit hypothesis of modularity is the same as the shape subset with the greatest difference in evolutionary rate. Here, we develop a new phylogenetic comparative method for comparing evolutionary rates among high-dimensional traits, and apply this method to analyze body shape evolution in bioluminescent lanternfishes. We frame the study of evolutionary rates and modularity through analysis of three hypotheses derived from the literature on fish development, biomechanics, and bioluminescent communication. We show that a development-informed partitioning of shape exhibits the greatest evolutionary rate differences among modules, but that a hydrodynamically informed partitioning is the best-fit modularity hypothesis. Furthermore, we show that bioluminescent lateral photophores evolve at a similar rate as, and are strongly integrated with, body shape in lanternfishes. These results suggest that overlapping life-history constraints on development and movement define axes of body shape evolution in lanternfishes, and that the positions of their lateral photophore complexes are likely a passive outcome of the interaction of these ecological pressures.

KEY WORDS: **Deep sea, fishes, geometric morphometrics, morphological evolution, phylogenetic comparative methods.**

The study of how anatomy changes through time unifies disparate areas of evolutionary biology (Darwin 1859; Simpson 1944), from quantitative genetics to paleontology. A concept that has emerged from this multifaceted study of anatomical change is that anatomy exhibits modular structure—that different character groups exhibit tight integration within clusters, and lower integration among clusters. Yet although evolutionary change is generally recognized to produce such patterns of modular organization through the interaction of function, development, and ecology (Wagner 1996; Wagner and Altenberg 1996; Klingenberg 2008), the macroevolutionary implications of modular organization are only beginning to be understood through studies combining hypothesis tests of modularity with inferred rates of morphological evolution (Goswami 2006; Wagner et al. 2007; Márquez 2008;

EVOLUTION
INTERNATIONAL JOURNAL OF ORGANIC EVOLUTION

Table 1. Hypotheses of modularity examined in this study, with landmark designations for each hypothesis and the predictions of each hypothesis with respect to relative rates, covariation, and modularity.

		Predictions		
Hypothesis	Landmarks in set	Rates	Covariation	Modularity
Growth gradients (H1)	**M1**: 1–9, 14, 18–23	$\sigma^2_{M1} > \sigma^2_{M2}$	–	H1
	M2: 10–13, 15–17			
Maneuverability/acceleration (H2)	**M1**: 1–9	$\sigma^2_{M1} \neq \sigma^2_{M2}$	–	H2
	M2: 10–23			
Information 1 (H3a)	**M1**: 1–4, 8–10, 12–14, 21–23	$\sigma^2_{M1} < \sigma^2_{M2}$	Strong	H3
	M2: 5–7, 11, 15–20			
Information 2 (H3b)		$\sigma^2_{M1} = \sigma^2_{M2}$	Weak or none	No prediction
Information 3 (H3c)		$\sigma^2_{M1} = \sigma^2_{M2}$	Strong	H1 or H2

Sanger et al. 2012; Claverie and Patek 2013; Goswami et al. 2014). Evolutionary rates and modularity provide insight into evolutionary processes. Rates of morphological evolution provide insight into function and ecology. For example, shifts in rates may affect both diversity and disparity in traits (Foote 1997; Harmon et al. 2003; Sidlauskas 2008), and differences in rates may reflect both changes in ecological niche (Simpson 1944; Harmon et al. 2010; Mahler et al. 2010) and differences or changes in trait functional groups (Price et al. 2010, 2013; Holzman et al. 2012; Collar et al. 2014). Moreover, such differences have been hypothesized to alter the selective regimes favoring different modules (Wagner et al. 2007; Clune et al. 2013), suggesting that novel trait functions can alter modularity at macroevolutionary scales. Yet in studies combining rates and modularity, such interactions have been traditionally downplayed; modules are normally treated as fixed, a priori hypotheses (e.g., Klingenberg 2009). Trait boundaries are defined by these modularity hypotheses, and the evolutionary rates of these traits are then estimated. However, the greatest morphological evolutionary rate differences across a shape may not align with a priori hypotheses of modularity because of the temporal disconnect between ecological response and the underlying architecture, and understanding how these patterns align or not can provide fundamental information about competing demands on organismal structure and potential macroevolutionary change. We therefore ask a fundamental question linking evolutionary rates and modularity—do body regions with the maximal difference in evolutionary rates agree with the body regions identified as the optimal hypothesis of modularity? This question addresses the traditional assumption that functional modules shape patterns of evolutionary rates (Wagner et al. 2007; Drake and Klingenberg 2010). To address this question, we develop a new phylogenetic comparative method for analyzing rates of multiple high-dimensional traits such as shape, and apply the method to compare the congruence of evolutionary rate regimes and modularity of three alternative hypotheses from the literature related to development, movement, and communication in midwater lanternfishes (Table 1).

For this study of rates and modules, we examine lanternfishes in the sister tribes Myctophini and Gonichthyini sensu Paxton, 1972. The midwater (mesopelagic) and upper bathypelagic environment imposes competing demands on organismal structure and function, including balancing demands on visual signal detection and production with increased crypsis, and decreased metabolic rate and increased locomotory capacity (Drazen and Seibel 2007). Because this region is populated by organisms with disparate body plans (Pietsch and Orr 2007) that suggest high degrees of modularity and/or high evolutionary rates of shape, these organisms are especially suited for analysis of the interplay between rates and modularity, and are particularly promising for understanding the assembly of morphological variation in the open ocean.

Among midwater organisms, lanternfishes (family Myctophidae) are an excellent example of the potential interplay between modularity and rates. Lanternfish body shapes span much of the morphospace occupation commonly seen in fishes (Claverie and Wainwright 2014), from dorsoventrally compressed and caudally elongated "slendertails," to lobate, "pumpkinseed" body shapes. In addition to exhibiting diverse body shapes, lanternfishes possess nine discrete postcranial bioluminescent photophore complexes, arranged in both outward facing (lateral) and downward facing (ventral) groups. Previous studies have hypothesized that such bioluminescent structures and mechanisms in midwater marine taxa function as key innovations (Van Valen 1971) or cohesion mechanisms in a region of the marine environment with limited allopatric boundaries (Haddock et al. 2010; Widder 2010; Davis et al. 2014). However, previous studies have failed to account for body shape as a covariate with bioluminescent structures in considering the role of bioluminescence in diversification processes (Davis et al. 2014), and so the nature of interaction between body shape and bioluminescent structures remains unknown. Changes in body shape, trophic characters,

or other biomechanical traits or ecological opportunity, shown to promote speciation in other taxa (Nosil 2012; Wagner et al. 2012), may instead be the predominant factors in midwater diversification, especially considering that bioluminescent structures may mature long after the developmental positioning of other metabolism- and locomotion-related traits (Moser and Ahlstrom 1970; Moser et al. 1984) that influence vagility or trophic displacement have constrained the final placement of such luminous organs. The configurations of bioluminescent structures such as those in lanternfishes may thus instead reflect the signature of interactions between evolutionary rate regimes and modularity. The wealth of character data for lanternfishes (Clarke 1973; Hartmann and Clarke 1975; Hulley and Krefft 1985; de Busserolles et al. 2013a,b, 2014; Poulsen et al. 2013; Denton 2014) allows explicit hypotheses regarding the interactions between body shape modularity, evolutionary rate regimes, and bioluminescent organs to be tested.

Hypotheses of Modules

We tested three alternative modularity hypotheses from the literature on teleost development and ecology, and lanternfish evolution: a *growth-gradients hypothesis* (H1), a *maneuverability/acceleration hypothesis* (H2), and an *information hypothesis* (H3). The growth-gradients hypothesis (Fuiman 1983) is a hypothesis of developmental modularity sensu Klingenberg (2008) derived from the observation that in some marine and freshwater larval fishes cranial and caudal morphology develop more rapidly than trunk morphology before transformation to the juvenile stage. This pattern is suggested to be driven by pressures promoting effective swimming (caudal elongation) and metabolic efficiency (gill arch and cranial development) during maturation. Lanternfish larvae comprise a large proportion of the mixed marine ichthyoplankton (Ahlstrom and Moser 1976; Loeb et al. 1993), but they descend out of it for larval transformation (Sassa et al. 2007). Therefore, different evolutionary rates in the cranial and caudal regions of different lanternfish species may reflect selection for temporal partitioning of larvae to mature at different times, resulting in separation of potential competitors, and in ecological differentiation across these fishes. In short, the growth-gradients hypothesis assumes that the greatest differences in evolutionary rates of shape align with developmental modules, and predicts that the functionally coupled cranial and caudal regions should evolve more rapidly than the body midsection. This hypothesis therefore assumes that metabolic and locomotory considerations, not bioluminescence, are the major determinants of evolutionary rates in lanternfish body shape, and that bioluminescent photophore patterns are established along axes defined by these constraints. This hypothesis is supported by the observation that all postcranial photophores in the lanternfishes studied here develop after larval transformation is complete (Moser and Ahlstrom 1970).

By contrast, the maneuverability/acceleration hypothesis (Webb 1984) is a hypothesis of functional modularity sensu Klingenberg (2008), and describes the scenario in which anterior morphology (cranium, oral jaws, and pectoral fin region) evolves at a different rate than posterior morphology (dorsal fin, trunk, anal fin, caudal fin, and peduncle), as might be predicted based on the hydrodynamics and theoretical modeling of adult swimming form and performance in fishes (Lauder and Tytell 2005). In fishes, the location, orientation, and size of the pectoral fins influences fine control features of swimming kinematics, including stationary rotation and rapid directional changes during forward movement. Similarly, the length and depth of the caudal peduncle and fin influences performance and metabolic efficiency of both continuous and burst/glide patterns of forward movement (Weihs 1974; Webb 1984; Blake 2004). These functional constraints on locomotory capacity are a general feature of fish body shape evolution, and may be prevalent in lanternfishes given the predation pressures faced by these fishes from both above and below. The maneuverability/acceleration hypothesis assumes that the greatest differences in the evolutionary rates of shape align with functional modules, but makes no specific prediction about which module should evolve more rapidly. Like the growth-gradients hypothesis, this hypothesis assumes that energetic and locomotory constraints, not bioluminescence, shape evolutionary rates of lanternfish body form.

Finally, the information hypothesis is a hypothesis of evolutionary modularity that predicts lateral body photophores evolve at a different rate than overall body shape. Previous studies have suggested the information hypothesis applies to lateral photophores, by noting lateral photophores are taxonomically informative at the generic and sometimes species level (Fraser-Brunner 1949; Paxton 1972), and by inferring a link between species richness and patterns of morphospace disparity by a subset of lateral photophores (Davis et al. 2014). However, these studies either did not include body shape as a covariate for photophore shape disparity (Davis et al. 2014), or considered only relative photophore positions without quantifying shape as a high-dimensional trait. Quantifying both body shape and lateral photophores together in such a way is crucial for accurately testing the information hypothesis because there is some support for both an informational and functional role for lateral photophores. For example, during feeding, many lanternfishes assort into species- and size-specific shoals (Tsarin 1999), and some lanternfish species exhibit modified lentiform scale coverings over lateral photophores (Lawry Jr. 1973) suggestive of adaptations for focusing the source of light output. Similarly, optic specializations in the retinas and photoreceptors of many lanternfish species, especially those in the tribes studied here, exhibit significant

modifications for detecting bioluminescent wavelengths (Turner et al. 2009; de Busserolles et al. 2013a,b, 2015). Specializations in both signal transmission and signal detection support an informational role for photophores in lanternfishes. By contrast, observational studies of lanternfish bioluminescence have noted that both the ventral (downward-facing) and lateral photophores light together (Barnes and Case 1974) when these fishes modulate their bioluminescent output for counterillumination, relative to ambient light conditions (Lawry Jr. 1974; Case et al. 1977), suggesting that lateral photophore luminescence may be induced by ambient light cues as much as by informational cues.

To distinguish between functional and informational roles of the interplay of photophores and body shape, we further subdivide the information hypothesis into three formulations by relating predictions of evolutionary rates with the direction of covariation implied by each formulation.

In the first formulation of the information hypothesis (H3a), photophores may evolve more rapidly than body shape, exist as distinct modules, and exhibit strong signal in a single axis of covariation relating changes in body shape to changes in photophore configuration. This pattern may be observed if lateral photophores inform on body shape and size, and if photophores are under disruptive selection to separate species of a given adult size class and ecological niche. This formulation of the information hypothesis assumes photophores and visual/recognition considerations drive shape evolution in lanternfishes.

In the second formulation of the information hypothesis (H3b), photophores may evolve at a rate similar to body shape, but possess no signal of covariation with body shape. This pattern may be observed if lateral photophores possess a purely functional role, such as for prey detection and startling, or predator evasion (Haddock et al. 2010), rather than an informational role (Davis et al. 2014). In this case, the lateral position of photophores only functions to project light outward from the body, and hence the specific configuration of the organs is irrelevant. This formulation of the information hypothesis assumes no link between photophores and body shape.

In the third formulation of the information hypothesis (H3c), photophores evolve at a rate similar to body shape, but also possess a strong axis of covariation with body shape. This pattern may be observed if lateral photophore position informs on body shape and size, but the position of lateral photophores is a function of factors related to body shape.

To test the predictions of these hypotheses, both high-dimensional data and high-dimensional methods are necessary. We therefore develop and implement a new comparative method for quantifying and assessing statistical significance of evolutionary rates in multiple high-dimensional traits, and use the method to estimate evolutionary rate differences for the three hypotheses of body form evolution in lanternfishes. We also estimate clade-specific evolutionary rates for the hypothesis with maximal rate difference in subsets. To assess congruence in modularity patterns and rate differences, we compare the maximal rate difference subset to the estimated best-fit hypothesis of modularity.

Methods

SPECIMENS AND MORPHOLOGICAL DATA

We characterized body shape from 33 species of lanternfish from the nominal tribes Myctophini and Gonichthyini sensu Paxton (1972). A total of 741 adult specimens were photographed, with an average of 22 individuals per species. Body shape was quantified using landmark-based geometric morphometric methods (Bookstein 1991; Mitteroecker and Gunz 2009; Adams et al. 2013). These methods quantify the shape of anatomical objects from the coordinates of landmark locations, after the effects of nonshape variation (position, orientation, and scale) have been mathematically held constant. Images of the left-lateral side of each specimen were obtained using a Nikon D3000 digital SLR camera with an AF-S Micro Nikkor 60mm 1:2.8 G ED lens, storing uncompressed NEF images at 4928 $\times$ 3264 pixels and exported as 16bit TIFF. The positions of 23 two-dimensional landmarks, representing a combination of overall body shape and photophore position, were digitized in tpsDig2 (Rohlf 2010). Sampled points were selected to capture variation among features related to body shape, caudal peduncle morphology, and medial fin positions (Fig. 1), which are known to be related to locomotion and maneuverability (Webb 1984). Points were also selected to capture features of the lateral luminous organs, which have been suggested to be related to visual detectability and species-specific cohesion (Davis et al. 2014). Specimens were aligned using generalized Procrustes superimposition (Rohlf and Slice 1990), and Procrustes tangent coordinates were treated as a set of shape variables for each specimen. The mean shape for each specimen was also calculated for the phylogenetic analyses below.

TIME-CALIBRATED PHYLOGENY

We generated a time-calibrated molecular phylogeny of tribes Myctophini and Gonichthyini sensu Paxton (Paxton 1972) based on six nuclear protein-coding genes (*histone H3*, *glyt*, *myh6*, *bmp4*, *tbr1*, and *zic1*) derived from a comprehensive study of myctophiform phylogeny (Denton 2014), with seven outgroup taxa from within the order Myctophiformes. Sampling of the ingroup was greater than 50% complete, with the species-level coverage among clade groupings, as defined in Denton (2014), as follows: *Benthosema* + *Diogenichthys* (87.5%), *Myctophum* sensu stricto (100%), *Hygophum* (44%), *Symbolophorus* (50%), *Loweina* + *Tarletonbeania* + *M. phengodes* (50%), *Centrobranchus* + *Gonichthys* (50%), and *Myctophum* sensu *Dasyscopelus* (70%).

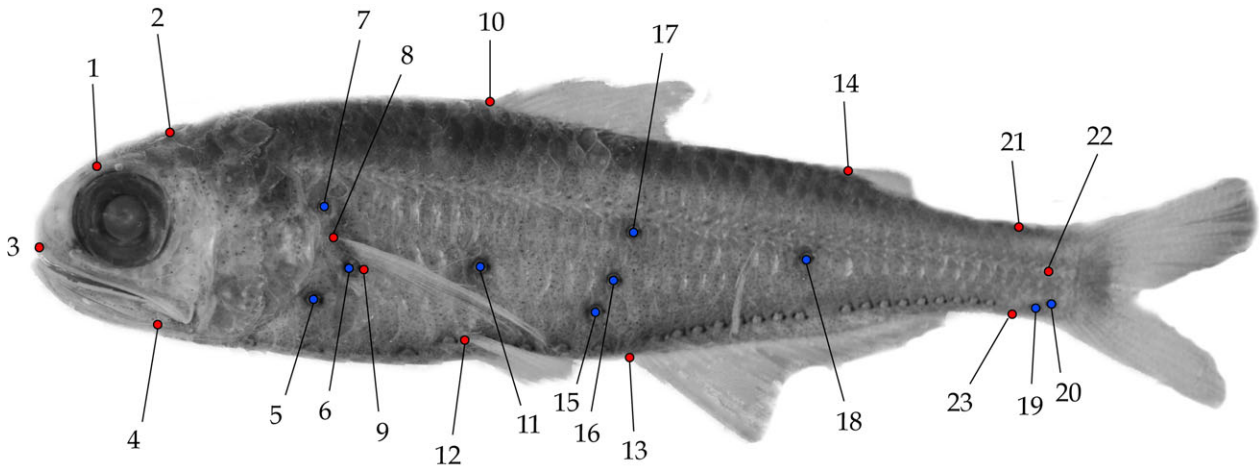

Figure 1. Landmark designations in this study, exemplified on *Myctophum punctatum* (MCZ105667), with anatomical elements of numbered landmarks as follows: (1) junction of frontal with orbit, (2) posterior of neurocranium, (3) anterior cusp of premaxilla, (4) posteriormost base of the dentary, (5) subpectoral (PVO) photophore 1, (6) PVO photophore 2, (7) suprapectoral (PLO) photophore, (8) anterodorsal insertion of pectoral fin, (9) posteroventral insertion of pectoral fin, (10) anterior insertion of dorsal fin, (11) supraventral (VLO) photophore, (12) anterior insertion of pelvic fin, (13) anteriormost insertion of anal fin, (14) anteriormost insertion of adipose fin, (15) supra-anal (SAO) photophore 1, (16) SAO photophore 2, (17) SAO photophore 3, (18) posterolateral (Pol) photophore, (19) precaudal (Prc) photophore 1, (20) Prc photophore 2, (21) anterodorsal insertion of procurrent caudal rays, (22) base of hypural plate, junction of dorsal and ventral hypurals, (23) anteroposterior insertion of ventral procurrent caudal rays.

Optimal data partitioning in PartitionFinder (Lanfear et al. 2012) using the BIC (Schwarz 1978) with unlinked branch lengths selected a (1, 2) + (3) codon position partitioning scheme, with HKY85 + Γ and K3Puf + Γ models, respectively. Divergence time estimation was conducted in BEAST version 1.8.1 (Drummond et al. 2012) using separate random local clocks (Drummond and Suchard 2010) and lognormal priors on three node fossil calibrations (†*Oligophus moravicus*, Gregorová 2004: $\mu = 1.5$, $\sigma = 0.5$, offset = 30; †*Myctophum columnae*, Sauvage 1873: $\mu = 1.5$, $\sigma = 0.5$, offset = 5.0; †*Eomyctophum sp.*, Giusberti et al. 2014: $\mu = 1.4$, $\sigma = 0.6$, offset = 46). The continuous-time Markov chain (CTMC) rate reference (Ferreira and Suchard 2008) was used as the prior for clock rates. A birth-death process with incomplete sampling correction (Gerhard 2008) was used as the tree prior. Analysis was run for 75 million generations, and was examined in Tracer version 1.6 for postburnin parameter effective sample size (ESS) values >200 to support convergence of the chain. A maximum clade credibility tree with node 95% highest posterior density (HPD) intervals was generated in TreeAnnotator version 1.8.1 (Fig. 2). The final tree was pruned to include only taxa for which morphological data were available.

COMPARING RATES AMONG PARTITIONS OF A HIGH-DIMENSIONAL TRAIT

The past decade has seen rapid developments in conceptual and analytical tools aimed at understanding both the covariation patterns within shape that underlie modularity (Magwene 2001; Márquez 2008; Klingenberg 2009), and the tempo and mode of morphological evolution in the context of evolutionary history (O'Meara et al. 2006; Felsenstein 2012; FitzJohn 2012; Adams 2013; Revell 2013; Adams 2014c; Rabosky 2014). Studies have combined analyses of modularity and rates by assessing modularity hypotheses and then evolving the major principal components of shape under Brownian motion (Sanger et al. 2012), or by calculating σ^2 using the Procrustes distances of species values from overall shape configurations (Claverie and Patek 2013). However, characterization of evolutionary rates for high-dimensional traits like modules requires a multidimensional perspective that accounts for both differences in trait dimension and phylogenetic history (Adams 2014c). To date, few studies have integrated analysis of evolutionary rates of shape and analysis of shape modularity using a multidimensional framework that characterizes trait variances, covariances, and multidimensional evolutionary rates. Below, we describe such a framework.

Recently, several approaches have been developed for comparing evolutionary rates among univariate traits in a phylogenetic context (Adams 2013), as well as for estimating and comparing phylogenetic evolutionary rates for high-dimensional traits among clades (Adams 2014c). Here, we combine the underlying logic of these two approaches and extend the multivariate method (Adams 2014c) for the comparison of phylogenetic evolutionary rates between multiple high-dimensional phenotypic traits. Such multivariate traits may represent distinct phenotypic components (e.g., body shape and head shape), or may be biological partitions or modules (sensu Olson and Miller 1958; Wagner 1996;

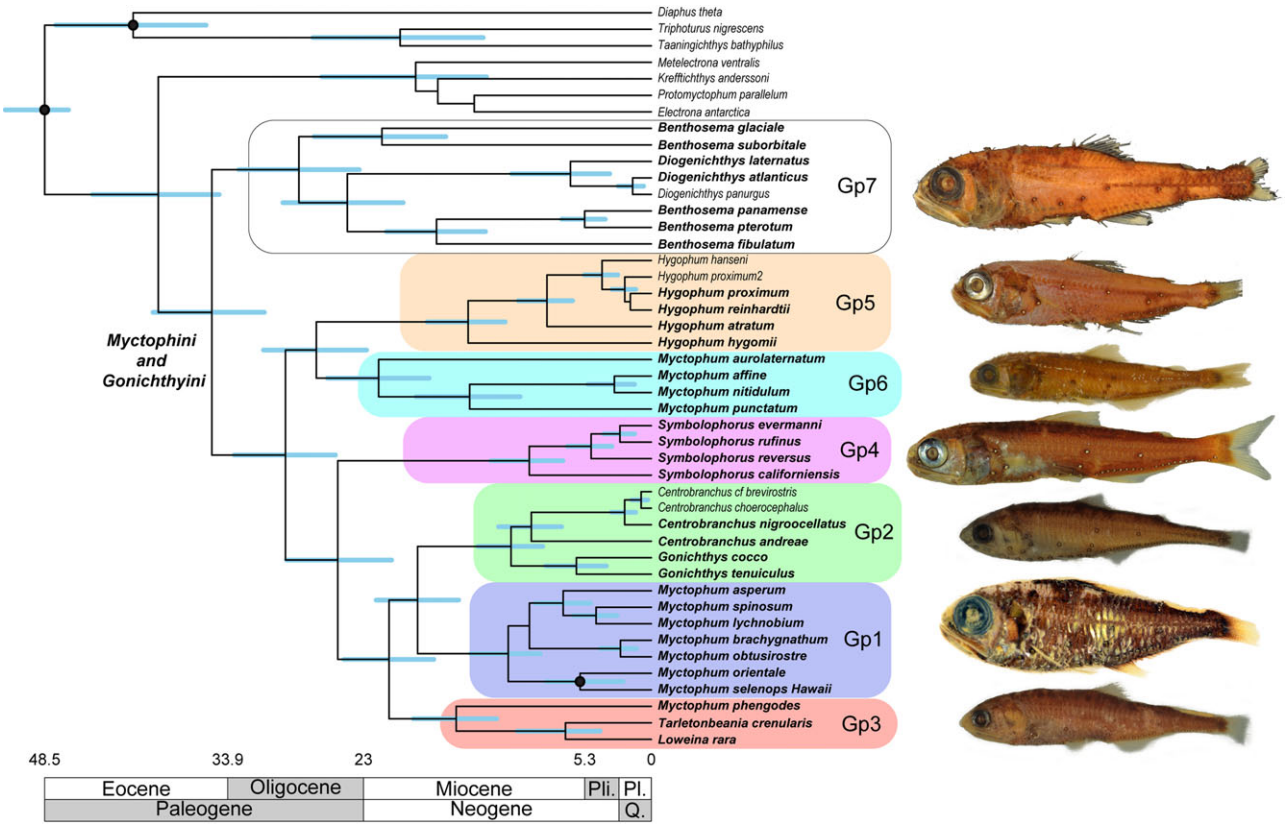

Figure 2. **Time-calibrated phylogeny of Myctophini and Gonichthyini sensu Paxton. Blue bars indicate 95% HPD intervals. Black dots indicate locations of fossil node calibrations (see main text for details). Taxa in bold are those with corresponding morphometric data. Specimen images represent the diversity in body shapes within the tribes and are, from top to bottom, *Benthosema glaciale* (MCZ125909), *Hygophum hygomii* (MCZ115714), *Myctophum aurolaternatum* (SIO61-57-25A), *Symbolophorus veranyi* (MCZ111606), *Centrobranchus andreae* (MCZ146602), *Myctophum selenops* (FMNH64619), and *Loweina rara* (MCZ102762). Group numberings mark clade designations in this study.**

Klingenberg 2009) within a single high-dimensional dataset. As with previous methods, the multivariate rate for each trait (σ^2_{mult}) is found under the assumption of evolution by Brownian motion (Felsenstein 1973, 2004).

To obtain an estimate of the evolutionary rate for a high-dimensional trait, we first obtain an $N \times p$ phenotypic trait matrix (**Y**), where each row contains the multivariate phenotypic mean for each of the N species. Next, the phylogenetic covariance matrix (**C**) is decomposed into its eigenvectors (**U**) and eigenvalues (**W**), and the phylogenetic transformation matrix **P** (following Adams and Collyer 2015) is constructed as: $\mathbf{P} = (\mathbf{U}\mathbf{W}^{1/2}\mathbf{U}^t)^{-1}$ (Garland Jr. and Ives 2000; Adams 2014b,c). Using this matrix, the multivariate phenotypic data are then transformed by the phylogeny as:

$$\mathbf{U}_\mathbf{Y} = (\mathbf{Y} - E(\mathbf{Y}))\mathbf{P}, \tag{1}$$

where **Y** is the matrix of phenotypic traits for all species and $E(\mathbf{Y})$ is an $N \times p$ matrix of the multivariate phylogenetic mean at the root of the phylogeny. From the phylogenetically transformed data, the Euclidean distance of each species relative to the origin is obtained, and these are assembled into an N x 1 vector ($\mathbf{PD}_{U,0}$). Finally, the net evolutionary rate for the multidimensional trait is calculated as:

$$\sigma^2_{mult} = \frac{\mathrm{PD}^t_{U,0}\mathrm{PD}_{U,0}}{Np}. \tag{2}$$

To compare evolutionary rates among two or more subunits, **Y** is first divided into submatrices ($\mathbf{Y}_K$), where K matrices represent the phenotypic data for each of the a priori anatomical subunits. The evolutionary rate for each subunit (σ^2_{pi}) is then found using equation (2), and the evolutionary rate ratio among subsets is then calculated as

$$R = \frac{\max(\sigma^2_{pi} \in \sigma^2_K)}{\min(\sigma^2_{pi} \in \sigma^2_K)}, \tag{3}$$

where σ^2_K is the set of evolutionary rates for each of the K subunits. To assess the statistical significance of this rate ratio, a simulation is performed under the null hypothesis of no rate difference between groups (i.e., under the hypothesis that a single

evolutionary rate is present for all subunits). To obtain values under this hypothesis, we first obtain the evolutionary rate for all traits (σ^2_{all}), as well as the evolutionary rate matrix (**R**) for the combined data. We then generate a common rate matrix for all traits, using (σ^2_{all}) along the diagonal of **R** (if required, this new matrix is adjusted slightly to conform to the properties of a valid covariance matrix). We then use this single rate model to simulate data along the phylogeny. For each simulated dataset, the rate ratio (R_{rand}) is then obtained, and the proportion of simulated ratios greater or equal to the observed is treated as the significance level of the observed value (Adams 2014c). We evaluated the statistical performance of the method proposed here using computer simulations under a Brownian motion model of evolution. From these simulations we confirmed that the approach has appropriate type I error rates and high statistical power, and is thus a valid procedure for evaluating rate differences among high-dimensional traits (see Supplementary Material). Additionally, the method is insensitive to increasing levels of trait covariation within modules, and is also insensitive to misspecification of landmarks to modules (Supplementary Material).

There is one additional consideration when using the procedure above to compare evolutionary rates among subsets of geometric morphometric data: whether the traits examined are derived from a single structure or multiple structures. If the traits are derived from a single trait (i.e., they represent subsets of landmarks from the same configuration), then a single Procrustes superimposition is first performed on all landmarks, followed by landmark partitioning and subsequent analysis. In this case, the procedure described above is used without alteration. However, if the shapes are derived from different structures each of which is superimposed separately, then differences in the number of landmarks in each structure must be taken into account because these can have a substantial effect on the resulting evolutionary rates and their comparison. In this case, the denominator of equation (2) is replaced by N, rather than $N\,x\,p$ (see Supplementary Material).

For the empirical dataset examined here, all landmarks were subjected to a single Procrustes superimposition, so the protocol was implemented as described above. Then, for each of the three hypotheses, landmarks were partitioned into modules (Table 1, Fig. 3A–C), and the evolutionary rates for each module were evaluated using the relative rate procedure above. Additionally, to evaluate the sensitivity of our rate estimates to intraspecific variation, we performed a bootstrap analysis in which pseudosamples representing the specimens within each species were obtained via bootstrapping (resampling with replacement), and a mean for the species was calculated, and used to estimate the evolutionary rates using equation (1). This procedure was replicated 1000 times to obtain a distribution of rates for each module, which could be compared to the rate based on the original sample of specimens.

Finally, to examine consistency of the relative rate magnitudes and to examine differences in evolutionary rate ranges between modules, we conducted clade-specific analysis. Clade designations were assigned following Denton (2014). We first split the modules into separate clade groups, and used the procedure of Adams (2014c) to test whether modules had significant differences among clades against the null hypothesis of no difference, using the relative rates procedure. To examine the effects of intraspecific variation, the procedure was repeated 10,000 times using the bootstrapping described above. Clade-specific rate ratios were calculated as the ratios (M1/M2) of the empirically estimated rates for each module. All analyses were performed in R (Team 2014) using the package *geomorph* (Adams and Otárola-Castillo 2013; Adams et al. 2014) and routines written by DCA.

SELECTING A BEST-FIT HYPOTHESIS OF MODULARITY

To assess a best-fit hypothesis of modularity for comparison to the hypothesis with the maximal difference in rate, we ranked modularity hypotheses using the γ^* statistic of Márquez (2008) in the software program MINT. To strengthen the assessment of difference between H1 and H3, a fourth model comprising three modules (prepectoral, trunk, and caudal) was amended to the model comparison. The resulting four models were compared against a null hypothesis of no modularity (H0). Strength of support for modularity hypothesis rankings based on γ^* was assessed using 100 replicates of jackknife procedure, removing 33% of specimens in each iteration.

INTEGRATION OF PHOTOPHORES AND BODY SHAPE

To quantify the direction and axes of integration between lateral photophores and body shape, a two-block phylogenetic partial least-squares (pPLS) analysis (Rohlf and Corti 2000; Adams and Felice 2014) was conducted in *geomorph*, assigning lateral photophores and body shape to separate blocks. Statistical significance of the inferred association was assessed using 10,000 rounds of permutation of landmark data from one block across the tips of the phylogeny against the null hypothesis of independence between the blocks. Because the pPLS procedure operates on individual measurements such as the group or species mean, the effect of intraspecific variation was accounted for by 10,000 rounds of resampling, using the procedure outlined for comparing rates.

Results

HYPOTHESES OF MODULAR EVOLUTIONARY RATES

Head + tail/trunk (growth-gradients) partitioning for M1 and M2 (H1, Table 1) exhibited the greatest difference in evolutionary rate ratio between modules ($R = 1.73$, $p = 0.0001$), a result

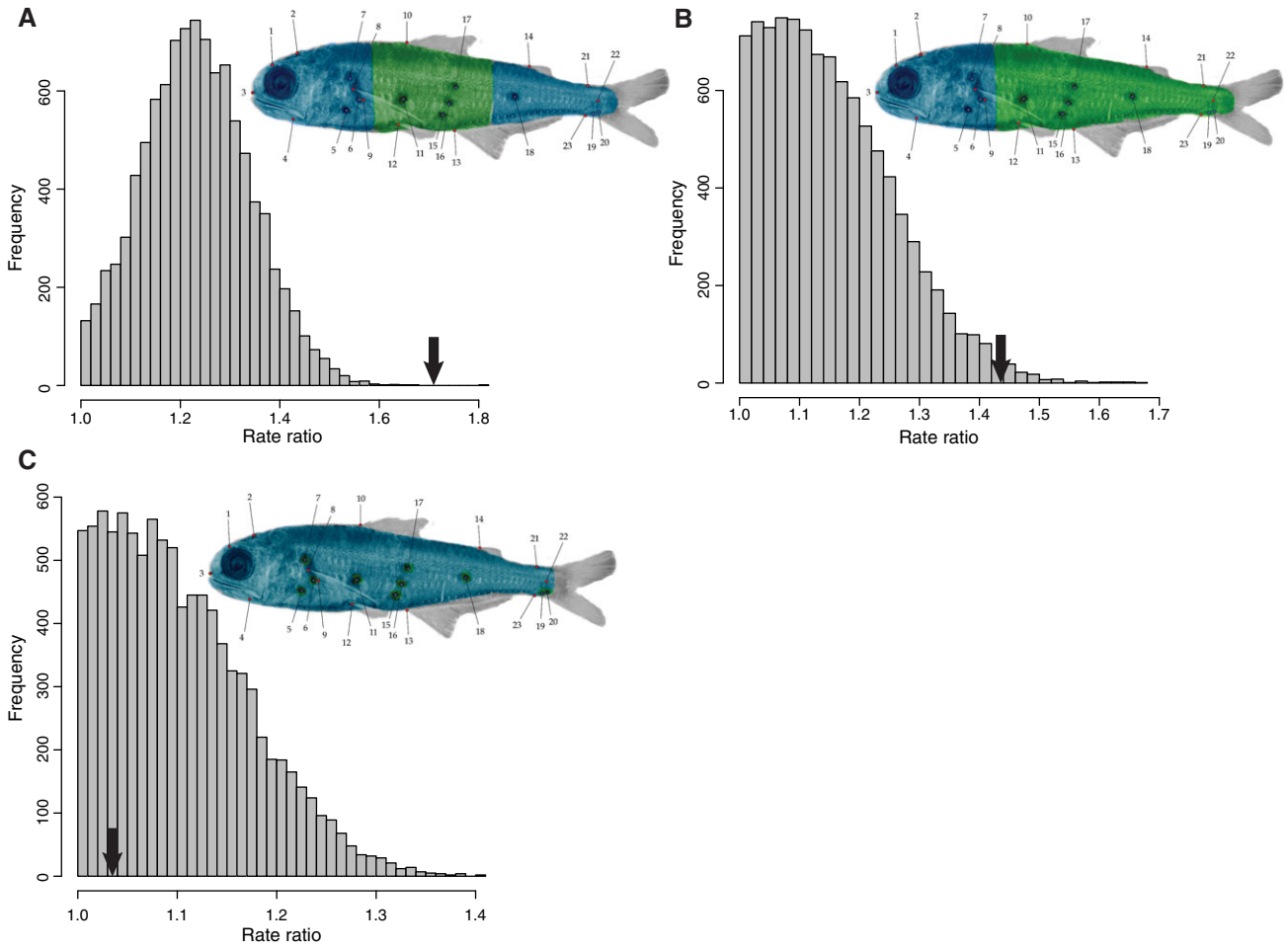

Figure 3. Results of permutation tests (N = 1000 iterations) of the deviation of modular rate ratios from unity for three a priori hypotheses. Colors corresponding to modules: M1 = blue, M2 = green, with landmark assignments given in Table 1 and Figure 1. Empirical rate ratios are indicated by the arrows. (A) H1, *growth-gradients* hypothesis, (B) H2, *maneuverability/acceleration* hypothesis, (C) H3, *information* hypothesis.

Table 2. Modular evolutionary rates, rate ratios, and statistical significance inferred for three a priori hypotheses of lanternfish morphological subsets.

Hypothesis	σ^2_{M1}	σ^2_{M2}	R	p-value, H	p-value, iv
H1	3.12×10^{-6}	5.38×10^{-6}	1.73 (1.67, 1.77)	1.00×10^{-4}	0.435
H2	3.11×10^{-6}	4.25×10^{-6}	1.37 (1.31, 1.42)	3.10×10^{-2}	0.417
H3	3.74×10^{-6}	3.88×10^{-6}	1.03 (1.00, 1.07)	0.781	0.542

Parameters and statistics for the models: σ^2_{M1} = evolutionary rate of module 1; σ^2_{M2} = evolutionary rate for module 2; R = rate ratio, plus interquartile range accounting for intraspecific variation; p-value, H = statistical significance of the deviation of the inferred rate ratio from unity; p-value, iv = statistical significance of intraspecific variation.

significantly different from the null hypothesis of similar rates (Table 2). The evolutionary rate magnitude for M1 ($\sigma^2_{M1} = 3.12 \times 10^{-6}$) was lower than the rate for the trunk ($\sigma^2_{M2} = 5.38 \times 10^{-6}$), a result opposite that predicted for rates by the growth-gradients hypothesis. Prepectoral/postpectoral (maneuverability/acceleration) partitioning for M1 and M2 (H2, Table 1) exhibited a smaller but also significant difference in evolutionary rate ratio between modules ($R = 1.37$, $p = 0.03$), rejecting the null hypothesis of similar rates.

By contrast, the information hypothesis (H3: $R = 1.03$, $p = 0.781$) exhibited no significant difference from unity, failing to reject the null hypothesis of similar evolutionary rates for photophores and body shape. The interquartile ranges of the rate ratios exhibited no overlap among hypotheses (Table 2, Fig. 3), and

intraspecific variation had no effect on the estimates of evolutionary rate ratios (H1: $p = 0.435$; H2: $p = 0.417$; H3: $p = 0.542$).

BEST-FIT MODULARITY HYPOTHESIS

The maneuverability/acceleration hypothesis (H2) was the best-fit modularity hypothesis ($\gamma^* = -0.2326$; 95% confidence interval (CI) = [−0.2429, −0.2225]), followed by the three-module ($\gamma^* = -0.149$; 95% confidence interval (CI) = [−0.1545, −0.143]), growth-gradients (H1) ($\gamma^* = -0.1029$; 95% confidence interval (CI) = [−0.1083, −0.0983]), and information (H3) ($\gamma^* = -0.0986$; 95% confidence interval (CI) = [−0.1035, −0.0942]) hypotheses. Jackknife resampling recovered H2 as the highest-ranking model in 100% of the replicates, followed by the three-module hypothesis (second best: 100%), H1 (third best: 88%), H3 (fourth best: 88%). The null hypothesis of no modularity ($\gamma^* = 0$) was rejected by ranking as the worst model in 100% of jackknife resamplings.

INTEGRATION OF PHOTOPHORES AND BODY SHAPE

The PLS correlation between photophores and body shape was significant (pPLS = 0.89194 ± 0.0107, $p < 0.0001$). This first dimension of shape covariation accounted for 83% of the total covariation (Fig. 4), and corresponded to changes in photophore position that reflected changes in body shape, including dorsoventral compression of the body profile, uniform decrease in the size of the cranial profile, and elongation and narrowing of the caudal peduncle, along with rostrad displacement of the SAO and Pol photophore complexes and caudad displacement of the Prc photophore complex with the caudal skeleton. Intraspecific variation had no effect on the measured value of the correlation ($p = 0.1008$).

CLADE-SPECIFIC MODULAR RATES

Estimation of clade-specific evolutionary rates (Table 3, Fig. 5) under the H1 subsets revealed distinct patterns related to both evolutionary rate ratios and to relative rate magnitudes. In nearly all clades, the trunk (M2) evolved approximately twice as quickly as the head/tail (M1), with clade-specific rate ratios (R_C) less than unity for all clades except *Myctophum s. str.* ($R_C = 1.111$). Across clades, evolutionary rate ratios of the head/tail (M1) ($R_C = 4.5$; $p = 0.001$) and trunk (M2) ($R_C = 6.02$; $p = 0.001$) were significantly different from unity, rejecting the null hypothesis of no difference in M1 and M2 rates among clades.

Clade-specific evolutionary rate magnitudes exhibited a wider range for the trunk (M2; range = 8.76×10^{-6}) than for the head/tail (M1; range = 3.89×10^{-6}). There was some evidence for consistent differences in overall evolutionary rate magnitudes in specific clades. The genus *Symbolophorus* exhibited some of the lowest evolutionary rate magnitudes for both subsets (M1 = 1.07×10^{-6}; M2 = 3.11×10^{-6}), and *Hygophum* exhibited some of the highest evolutionary rate magnitudes for both subsets (M1 = 4.94×10^{-6}; M2 = 1.09×10^{-5}).

Discussion

Our study asked two fundamental questions—first, do maximal differences in evolutionary rates among body shape regions align with the optimal hypothesis of modularity? Second, do bioluminescent organs play a role in shaping the interplay between shape evolutionary rates and modularity? The results of our study answer both questions. We show that: (1) the highest evolutionary rate differences within regions of a shape—rate modules—do not necessarily correspond to modules of shape covariation; and (2) bioluminescent lateral photophores evolve along the same axis, and at a similar rate, as body shape in lanternfishes, supporting nearly all the predictions of the third formulation of the information hypothesis (H3c), which predicted strong integration between photophores and body shape, optimality of a functional modularity hypothesis, and equal rates for photophores and body shape. The implications of these two results are discussed in turn.

RATE MODULARITY AND SHAPE COVARIATION

Studies of the macroevolutionary interplay of modularity and evolutionary rates of shape is complicated by the relationships among the concepts of modularity and integration (Klingenberg 2009, 2013; Klingenberg and Marugán-Lobón 2013), by the scale of analysis, in terms of both phylogenetic and anatomical coverage (Drake and Klingenberg 2010; Goswami and Polly 2010; Sanger et al. 2012; Claverie and Patek 2013; Goswami et al. 2014), and by differences in how the statistical and morphological quantities are measured (Márquez 2008; Klingenberg 2009; Smilde et al. 2009; Haber 2011). As a result, the relationships among these quantities are not always generalizable across different studies (Klingenberg 2014). This analysis develops a statistical framework for uniting modular evolutionary rates of shape with traditional inference of modularity in a common high-dimensional framework, and reveals for the first time a case of clear discrepancy between rate modules and modules of shape covariation (variational modules, sensu Wagner et al. 2007). Specifically, as shown in Table 2, our results reveal that the growth-gradients hypothesis (H1) exhibits a nearly twofold difference in evolutionary rates between the head/tail and trunk regions, but that the best-fit hypothesis of modularity corresponds to the function-coupled maneuverability/acceleration hypothesis (H2). Although genetic and functional modules have been shown to be potentially incongruent in their partitioning of phenotypic traits (Cheverud 1982; Atchley and Hall 1991; Magwene 2001; Klingenberg et al. 2003; Márquez 2008), the results of our study show for the first time that evolutionary rate modules and variational modules (e.g., Drake and Klingenberg 2010; Claverie and Patek 2013) can be incongruent

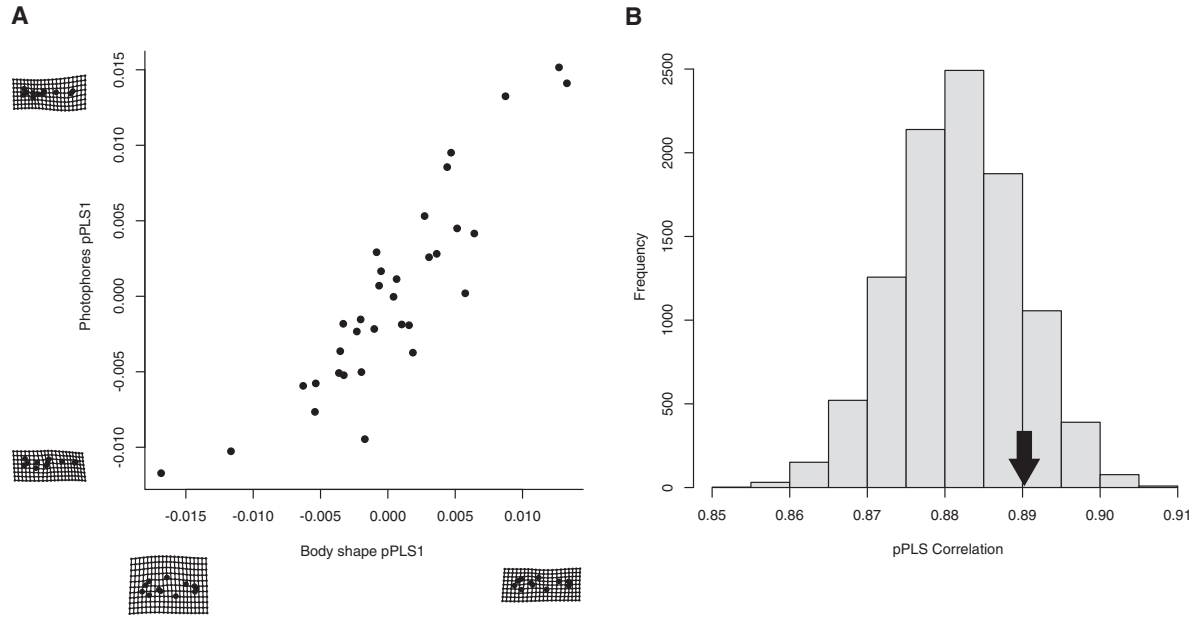

Figure 4. **Results of two-block phylogenetic partial least-squares (pPLS) analysis of body shape and photophores as separate blocks. (A) Approximately 83% of total covariation between body shape and photophore position was described by the first PLS axis, which related dorsoventral compression and caudal peduncle elongation to dorsoventral midline migration of trunk photophores. (B) Distribution of pPLS correlation values generated through resampling (N = 10,000 iterations) to account for intraspecific variation. The null hypothesis of no effect of intraspecific variation was not rejected.**

Table 3. **Modular evolutionary rates and rate ratios inferred for clades under H1.**

Clade	Label	$\sigma^2_{M1,c}$	$\sigma^2_{M2,c}$	R_C
Myctophum sensu *Dasyscopelus*	Gp1	2.96×10^{-6}	5.14×10^{-6}	0.576
Centrobranchus + *Gonichthys*	Gp2	4.96×10^{-6}	6.98×10^{-6}	0.71
Loweina + *Tarletonbeania* + *M. phengodes*	Gp3	4.09×10^{-6}	7.36×10^{-6}	0.556
Symbolophorus	Gp4	1.07×10^{-6}	3.11×10^{-6}	0.346
Hygophum	Gp5	4.94×10^{-6}	1.09×10^{-5}	0.453
Myctophum sensu stricto	Gp6	2.38×10^{-6}	2.14×10^{-6}	1.111
Benthosema + *Diogenichthys*	Gp7	2.21×10^{-6}	4.15×10^{-6}	0.532
Background	bg	3.09×10^{-6}	5.45×10^{-6}	0.567

Abbreviations as in Table 2.

as well. Rate modularity may therefore be considered a separate modularity pattern that requires exploration in tests relating variational modularity to evolutionary rates in macroevolutionary studies.

Moreover, our inferred pattern of discrepancy between rate and variational modules suggests the possibility that incipient changes in modularity may be inferable from phenotypic data when using similar high-dimensional approaches to test both quantities. Our new method is effectively a high-dimensional, phylogenetically standardized disparity measure for trait modules, and changes in patterns of morphological disparity may reflect shifting trait function (Collar et al. 2014) or shifts in ecological niche (Simpson 1944; Harmon et al. 2003). Such shifts may affect different parts of an organism (e.g., variational adaptation, Wagner et al. 2007), either as an adult, or during ontogeny (Leroi 2000; Fischer-Rosseau et al. 2009) by changing the selective regimes responsible for coupling or decoupling functional trait groups, or by altering what traits may evolve neutrally (Monteiro et al. 2005; Drake and Klingenberg 2010). As suggested from models for the evolution of modularity, differential ecological effects of different phenotypic trait groups may have direct fitness effects on modularity by changing the overall fitness (ratio of network performance to connection cost) of an existing modularity structure of connected components in the molecular and genetic networks underlying organismal traits (Clune et al. 2013). Alternatively, shifts in ecological niche may favor the emergence of modularity as an indirect effect of the specialization of gene function or activity patterns (Espinosa-Soto and Wagner 2010).

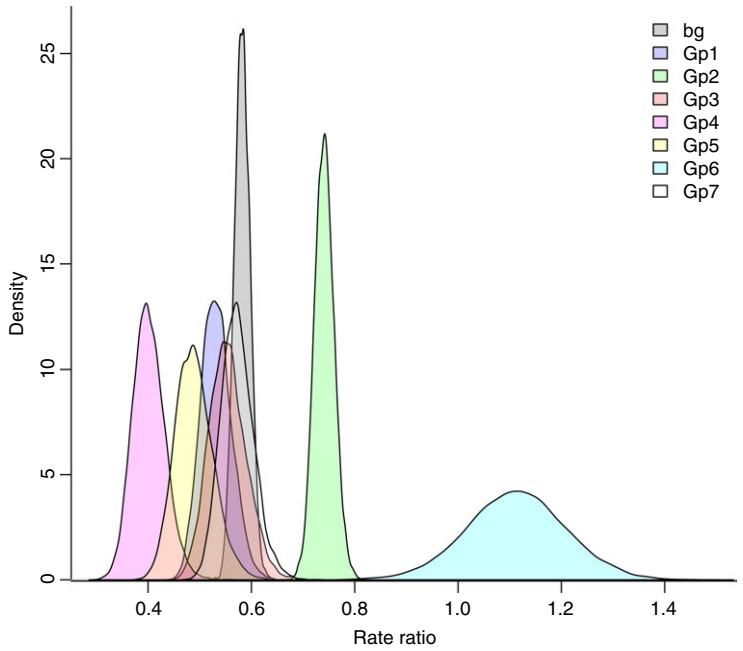

Figure 5. Results of clade-specific permutation tests ($N = 10{,}000$ iterations) under the *growth-gradients* hypothesis (H1). Distributions of evolutionary rate ratios for each clade account for intraspecific variation via resampling. Colors of density plots correspond to groups from Figure 2.

Therefore, identifying rate and variational module discrepancy may point to incipient changes in underlying variational modularity. Future studies may assess this prediction using comparative phylogenetic analysis of taxa for which developmental and transcriptomic data are known.

Incipient modularization in our study may further be implied from the inferred modularity model rankings. The maneuverability/acceleration hypothesis (H2) was selected as the best-fit modularity hypothesis in all jackknife replicates, but the three-module hypothesis (cranial, trunk, and caudal regions) was ranked second best in all jackknife replicates. The maneuverability/acceleration hypothesis is a functional hypothesis that is consistent with the hydrodynamic constraints imposed on fishes over the course of life history, and may thus be assumed to be an early-emerging and predominantly fixed modularity pattern across fishes, just as separate cranial and facial developmental modules are consistently observed across mammals (Goswami 2006; Drake and Klingenberg 2010; Goswami and Polly 2010). The strength of support for the three-module hypothesis suggests the possibility that the separation of the postpectoral region into separate trunk and caudal regions, a prediction of the growth-gradients hypothesis (H1), is the result of an incipient shift from two modules to three in lanternfishes. Although modularity is expected to increase through time (Wagner 1996; Wagner and Altenberg 1996), most existing studies of the evolutionary modularity have defined increases in modularity as the decrease in integration among a fixed set of modules (e.g., Claverie and Patek 2013), an analytical artifact of approaches using between-group measurements on a priori hypotheses. Increasing the number of modules is another way to increase modularity that is a novel result consistent with the assumptions. The caveat of our interpretation of incipient modularization is that functional modularity should select for variational modularity—that functional differences should result in concomitant changes in the underlying architecture over evolutionary time (Wagner et al. 2007).

The preceding discussion therefore assumes that the trunk has enough functional or developmental significance to induce a change in modularity. As shown in Tables 2 and 3, the trunk region (M2) exhibits a nearly twofold increase in both relative evolutionary rate and in evolutionary rate range (relative to M1) among clades (Fig. 5). Although we reject the null hypothesis of no difference among clades for M1 and M2 separately, elevated relative evolutionary rates and increased rate ranges in the trunk at first seem at odds with other studies recovering the most elevated evolutionary rates in cranial and other prey-processing traits related to resource partitioning and trophic divergence in fishes (Price et al. 2011, 2013; Holzman et al. 2012). Adults of the lanternfishes in the tribes studied here feed predominantly on similar zooplankton with significant trophic overlap (Hopkins and Gartner Jr. 1992; Pakhomov et al. 1996), making similar analogies of fine-scale resource partitioning among adult lanternfishes difficult to delineate. Instead, differences in trunk evolutionary rate magnitudes and ratios may reflect differences in the maturation time of the visceral organs, especially the gut and swimbladder,

and form the basis of the ecological divergence hypothesized by the growth-gradients hypothesis to instead be based on locomotion and respiration. Gut maturation in larval fishes generally occurs rapidly after the development of head and fins (Osse 1989), with the timing of exocrine organ development playing a significant role in determining prey type (Infante and Cahu 2001). Gut length in marine fishes is also strongly linked to prey type, and changes in relative gut length during larval development help determine the stage at which larval fishes can switch between prey types. Many lanternfish species in the tribes studied here exhibit differential elongation of the gut during larval development (Moser and Ahlstrom 1970), ranging from little elongation in *Hygophum* to extreme elongation in *Loweina* and in the trailing gut of *Myctophum* (*s. str.*) *aurolaternatum*. Therefore, the elevated rate range and relative rates in the trunk might reflect physical and biochemical differences in maturation related to a temporal, rather than morphological, resource partitioning (Sabatés and Saiz 2000) of the primarily ostracod prey on which lanternfish larvae in the tribes studied feed (Conley and Hopkins 2004).

PHOTOPHORES AND BODY SHAPE

Reviews of the deep-sea environment have often suggested bioluminescence to play the role of a key innovation by any number of potentially diversification-promoting mechanisms (Haddock et al. 2010), and this idea has been further supported by studies linking differential species diversity to increased disparity in lateral photophore patterns (Davis et al. 2014). Here, by quantifying both body shape and lateral photophore configuration as high-dimensional traits, our analysis moves beyond correlative study to address whether bioluminescent organ evolution exhibits a unique evolutionary signature independent of body shape (H3a; Table 1), as might be expected if lateral photophores were under disruptive selection to separate panmictic adults into different foraging or spawning assemblages. Our results instead suggest that the position of lateral photophores in lanternfishes may be a passive effect of the interaction between functional modularity and ecological divergence—the third formulation of the information hypothesis—manifested in body shape changes throughout the larval period. Specifically, as shown in the results of modularity hypothesis selection, and in Table 2 and Figure 3, there was negligible support for either variational or rate modularity in photophores and body shape. These results are consistent with the interaction of photophore and larval development: photophores are innervated by peripheral rami of spinal nerves (Ray 1950) whose positions are laid down during larval maturation. In the myctophinin and gonichthyine lanternfishes studied here, the lateral photophores emerge during or after larval transformation, and after major innervation has already taken place (Moser and Ahlstrom 1970, 1974; Moser et al. 1984).

Furthermore, as shown by the results of the two-block pPLS between photophores and body shape (Fig. 4), the overwhelming dimension of covariation between photophores and body shape reflected simple positional differences relating changes in body depth and caudal peduncle length to midline centralization in lateral photophore groups. This axis of covariation suggests an informational role for lateral photophores, and agrees with previous studies hypothesizing a possible role for these complexes in species-specific cohesion (Fraser-Brunner 1949; Paxton 1972; Davis et al. 2014). However, by demonstrating that modularity patterns in myctophinin and gonichthyine lanternfishes follow functional and developmental considerations and that photophores and body shape are not separable variational or rate entities in these tribes, our results somewhat decouple lateral photophores from the exceptional diversification rates inferred for this family (e.g., Near et al. 2014) in favor of a hypothesis that partitioning in overall developmental trajectories (e.g., caeogenetic development, McGinnis 1982) is both the determinant of photophore position and the factor underlying diversification by promoting fine-scale ecological partitioning during ontogeny (Sabatés and Saiz 2000; Conley and Hopkins 2004; Conley and Gartner Jr. 2009; Price et al. 2013). Although the results of our study are confined to members of nominal sister tribes within one of the lanternfish subfamilies, it is likely that the conclusions will be applicable across the family given the general congruence of lanternfish larval characters with phylogeny (Denton 2014).

Finally, by inferring strong covariation between photophores and body shape, our results reject the second formulation of the information hypothesis (H3b; Table 1), which predicted a functional role for lateral photophores, such as in startle response, as manifested in either weak covariation between photophore position and body shape, or in covariation spread over multiple significant axes. Rejection of this hypothesis in support of the third formulation instead suggests that the different complexes (lateral and ventral) in the innervated lanternfish photophore system may serve multiple simultaneous functions and thereby place potentially strong constraints on accuracy in detection of bioluminescent sources. This suggestion has been supported in recent studies of lanternfish vision (e.g., Turner et al. 2009), which have shown that species in the tribes studied here possess some of the most derived visual systems in the family, including both a variably positioned, sexually dimorphic intraocular filter and rhodopsin gene duplication (de Busserolles et al. 2015) and microtubule-like structures in the inner layer of the retina (de Busserolles et al. 2013b).

PHYLOGENETIC COMPARISONS OF RATES AMONG MULTIPLE HIGH-DIMENSIONAL TRAITS

Beyond our empirical findings, the work described here provides a critical extension to the phylogenetic comparative toolkit for

studying of rates of evolution in modular regions of a shared structure, and in comparing across different high-dimensional phenotypic shapes. This advance mirrors other recent developments of the phylogenetic comparative toolkit, which have endeavored to combine the mathematics of high-dimensional multivariate traits such as shape with recent macroevolutionary theory for examining trait evolution in a phylogenetic context. Much like the analysis of univariate traits, with these tools, one may now evaluate hypotheses that examine the degree of phylogenetic signal in multivariate traits (Adams 2014a), estimate their rates of phenotypic evolution (Adams 2014c), and examine evolutionary correlations for high-dimensional data (Adams 2014b; Adams and Felice 2014; Adams and Collyer 2015). Our approach builds on this growing body of multivariate macroevolutionary methods by enabling the comparison of rates of phenotypic evolution between multiple high-dimensional traits; thereby extending the phylogenetic comparative toolkit in yet another dimension.

ACKNOWLEDGMENTS

We thank the many institutions (standard abbreviation in parentheses) that provided collections access to specimens for morphometric analysis, including K. Hartel (MCZ), W. L. Smith (FMNH), B. Brown (AMNH), and H. J. Walker (SIO). For permission to use photos, we thank the Museum of Comparative Zoology, Harvard University (*Myctophum punctatum* MCZ105667, *Centrobranchus andreae* MCZ146602, *Loweina rara* MCZ102762, *Benthosema glaciale* MCZ125909, *Hygophum hygomii* MCZ115714, and *Symbolophorus veranyi* MCZ111606), H. J. Walker (*Myctophum aurolaternatum* SIO61-57-25A), and W. L. Smith (*Myctophum selenops* FMNH64619). Original MCZ specimen photographs are ©President and Fellows of Harvard College. This work was sponsored in part by National Science Foundation grant DEB-1209573 and by a Lerner-Gray Marine Research grant, both to JSSD, and in part by National Science Foundation grant DEB-1257287 to DCA. The authors claim no competing interests. Data Archival location: Supplementary methods, as well as datasets and R scripts supporting this article, have been uploaded as part of the Supplementary Material.

LITERATURE CITED

Adams, D. C. 2013. Comparing evolutionary rates for different phenotypic traits on a phylogeny using likelihood. Syst. Biol. 62:181–192.

———. 2014a. A generalized K statistic for estimating phylogenetic signal from shape and other high-dimentional multivariate data. Syst. Biol. 63:685–697.

———. 2014b. A method for assessing phylogenetic least squares models for shape and other high-dimensional multivariate data. Evolution 68:2675–2688.

———. 2014c. Quantifying and comparing phylogenetic evolutionary rates for shape and other high-dimensional phenotypic data. Syst. Biol. 63:166–177.

Adams, D. C., and M. L. Collyer. 2015. Permutation tests for phylogenetic comparative analyses of high-dimensional shape data: what you shuffle matters. Evolution 69:823–829.

Adams, D. C., and R. Felice. 2014. Assessing phylogenetic morphological integration and trait covariation in morphometric data using evolutionary covariance matrices. PLoS One 9:e94335.

Adams, D. C., and E. Otárola-Castillo. 2013. Geomorph: an R package for the collection and analysis of geometric morphometric shape data. Methods Ecol. Evol. 4:393–399.

Adams, D. C., M. L. Collyer, E. Otárola-Castillo, and E. Sherratt. 2014. geomorph: software for geometric morphometric analyses. R package version 2.1.2. Available at http://CRAN.R-project.org/package=geomorph. January 7th, 2015.

Adams, D. C., F. J. Rohlf, and D. E. Slice. 2013. A field comes of age: geometric morphometrics in the 21st century. Hystrix 24:7–14.

Ahlstrom, E. H., and H. G. Moser. 1976. Eggs and larvae of fishes and their role in systematic investigations and in fisheries. Revue des Travaux de l'Institut des Peches Maritimes 40:379–398.

Atchley, W. R., and B. K. Hall. 1991. A model for development and evolution of complex morphological structures. Biol. Rev. 66:101–157.

Barnes, A. T., and J. F. Case. 1974. The luminescence of lanternfish (Myctophidae): spontaneous activity and responses to mechanical, electrical, and chemical stimulation. J. Exp. Biol. Ecol. 15:203–221.

Blake, R. W. 2004. Fish functional design and swimming performance. J. Fish Biol. 65:1193–1222.

Bookstein, F. L. 1991. Morphometric tools for landmark data: geometry and biology. Cambridge Univ. Press, Cambridge, UK.

Case, J. F., J. Warner, A. T. Barnes, and M. Lowenstine. 1977. Bioluminescence of lantern fish (Myctophidae) in response to changes in light intensity. Nature 265:179–181.

Cheverud, J. M. 1982. Relationships among ontogenetic, static, and evolutionary allometry. Am. J. Phys. Anthropol. 59:139–149.

Clarke, T. A. 1973. Some aspects of the ecology of lanternfishes (Myctophidae) in the Pacific Ocean near Hawaii. Fish. Bull. 71:401–434.

Claverie, T., and S. N. Patek. 2013. Moduarity and rates of evolutionary change in a power-amplified prey capture system. Evolution 67:3191–3207.

Claverie, T., and P. C. Wainwright. 2014. A morphospace for reef fishes: elongation is the dominant axis of body shape evolution. PLoS One 9:e112732.

Clune, J., J.-B. Mouret, and H. Lipson. 2013. The evolutionary origins of modularity. Proc. R. Soc. Lond. B Biol. Sci. 280:20122863.

Collar, D. C., P. C. Wainwright, M. E. Alfaro, L. J. Revell, and R. S. Mehta. 2014. Biting disrupts integration to spur skull evolution in eels. Nat. Commun. 5:5505, 9 pages. doi 10.1038/ncomms6505.

Conley, W. J., and J. V. Gartner Jr. 2009. Growth among larvae of lanternfishes (Teleostei: Myctophidae) from the eastern Gulf of Mexico. Bull. Mar. Sci. 84:123–135.

Conley, W. J., and T. L. Hopkins. 2004. Feeding ecology of lanternfish (Pisces: Myctophidae) larvae: prey preferences as a reflection of morphology. Bull. Mar. Sci. 75:361–379.

Darwin, C. 1859. On the origin of species by means of natural selection, or the preservation of favoured races in the struggle for life. John Murray, London, U.K.

Davis, M. P., N. I. Holcroft, E. O. Wiley, J. S. Sparks, and W. L. Smith. 2014. Species-specific bioluminescence facilitates speciation in the deep sea. Mar. Biol. 161(5):1–10.

de Busserolles, F., J. L. Fitzpatrick, N. J. Marshall, and S. P. Collin. 2014. The influence of photoreceptor size and distribution on optical sensitivity in the eyes of lanternfishes (Myctophidae). PLoS One 9:e99957.

de Busserolles, F., J. L. Fitzpatrick, J. R. Paxton, N. J. Marshall, and S. P. Collin. 2013a. Eye-size variability in deep-sea lanternfishes (Myctophidae): an ecological and phylogenetic study. PLoS One 8:e58519.

de Busserolles, F., N. J. Marshall, and S. P. Collin. 2013b. The eyes of lanternfishes (Myctophidae, Teleostei): novel ocular specialisations for vision in dim light. J. Comp. Neurol. 522:1618–1640.

de Busserolles, F., N. S. Hart, D. M. Hunt, W. I. Davies, N. J. Marshall, M. W. Clarke, D. Hahne, and S. P. Collin. 2015. Spectral tuning in the eyes of deep-sea lanternfishes (Myctophidae): a novel sexually dimorphic intra-ocular filter. Brain Behav. Evol 85:77–93.

Denton, J. S. S. 2014. Seven-locus molecular phylogeny of Myctophiformes (Teleostei; Scopelomorpha) highlights the utility of the order for studies of deep-sea evolution. Mol. Phylogenet. Evol. 76:270–292.

Drake, A. G., and C. P. Klingenberg. 2010. Large-scale diversification of skull shape in domestic dogs: disparity and modularity. Am. Nat. 175:289–301.

Drazen, J. C., and B. A. Seibel. 2007. Depth-related trends in metabolism of benthic and benthopelagic deep-sea fishes. Limnol. Oceanogr. 52:2306–2316.

Drummond, A. J., and M. A. Suchard. 2010. Bayesian random local clocks, or one rate to rule them all. BMC Biol. 8:114.

Drummond, A. J., M. A. Suchard, D. Xie, and A. Rambaut. 2012. Bayesian phylogenetics with BEAUti and the BEAST 1.7. Mol. Biol. Evol. 29:1969–1973.

Espinosa-Soto, C., and A. Wagner. 2010. Specialization can drive the evolution of modularity. PLoS Comput. Biol. 6:e1000719.

Felsenstein, J. 1973. Maximum likelihood estimation of evolutionary trees from continuous characters. Am. J. Hum. Genet. 25:471–492.

———. 2004. Inferring Phylogenies. Sinauer Associates, Inc., Sunderland, MA.

———. 2012. A comparative method for both discrete and continuous characters using the threshold model. Am. Nat. 179:145–156.

Ferreira, M. A., and M. A. Suchard. 2008. Bayesian analysis of elapsed times in continuous-time Markov chains. Can. J. Stat. 36:355–368.

Fischer-Rosseau, L., R. Cloutier, and M. L. Zelditch. 2009. Morphological integration and developmental progress during fish ontogeny in two contrasting habitats. Evol. Dev. 11:740–753.

FitzJohn, R. G. 2012. Diversitree: comparative phylogenetic analyses of diversification in R. Methods Ecol. Evol. 3:1084–1092.

Foote, M. 1997. The evolution of morphological diversity. Annu. Rev. Ecol. Syst. 28:129–152.

Fraser-Brunner, A. 1949. A classification of the fishes of the family Myctophidae. Proc. Zool. Soc. Lond. 118:1019–1106.

Fuiman, L. A. 1983. Growth gradients in fish larvae. J. Fish Biol. 23:117–123.

Garland, T. Jr, and A. R. Ives. 2000. Using the past to predict the present: confidence intervals for regression equations in phylogenetic comparative methods. Am. Nat. 155:346–364.

Gerhard, T. 2008. The conditioned reconstructed process. J. Theor. Biol. 253:769–778.

Giusberti, L., A. F. Bannikov, F. Boscolo Galazzo, E. Fornaciari, J. Frieling, V. Luciani, C. A. Papazzoni, G. Roghi, S. Schouten, and A. Sluijs. 2014. A new *Fossil-Lagerstätte* from the Lower Eocene of Lessini Mountains (northern Italy): a multidisciplinary approach. Palaeogeogr. Palaeoclimatol. Palaeoecol. 403:1–15.

Goswami, A. 2006. Cranial modularity shifts during mammalian evolution. Am. Nat. 168:270–280.

Goswami, A., and P. D. Polly. 2010. The influence of modularity on cranial morphological disparity in Carnivora and Primates (Mammalia). PLoS One 5:e9517.

Goswami, A., J. B. Smaers, C. Soligo, and P. D. Polly. 2014. The macroevolutionary consequences of phenotypic integration: from development to deep time. Philos. Trans. R. Soc. B Biol. Sci. 369(1649):20130254, 15 pages.

Gregorová, R. 2004. A new Oligocene genus of lanternfish (family Myctophidae) from the Carpathian Mountains. Revue de Paléobiologie, Genève 9:81–97.

Haber, A. 2011. A comparative analysis of integration indices. Evol. Biol. 38:476–488.

Haddock, S. H. D., M. A. Moline, and J. F. Case. 2010. Bioluminescence in the sea. Ann. Rev. Mar. Sci. 2:443–493.

Harmon, L. J., J. A. Schulte, A. Larson, and J. B. Losos. 2003. Tempo and mode of evolutionary radiation in iguanian lizards. Science 301:961–964.

Harmon, L. J., J. B. Losos, T. J. Davies, R. G. Gillespie, J. L. Gittleman, W. B. Jennings, K. H. Kozak, M. A. McPeek, F. Moreno-Roark, and T. J. Near. 2010. Early bursts of body size and shape evolution are rare in comparative data. Evolution 64:2385–2396.

Hartmann, A. R., and T. A. Clarke. 1975. The distribution of myctophid fishes across the Central Equatorial Pacific Fishery Bulletin 73:633–641.

Holzman, R., D. C. Collar, S. A. Price, C. D. Hulsey, R. C. Thomson, and P. C. Wainwright. 2012. Biomechanical trade-offs bias rates of evolution in the feeding apparatus of fishes. Proc. R. Soc. B Biol. Sci. 279:1287–1292.

Hopkins, T. L., and J. V. Gartner Jr. 1992. Resource-partitioning and predation impact of a low-latitude myctophid community. Mar. Biol. 114:185–197.

Hulley, P. A., and G. Krefft. 1985. A zoogeographic analysis of the fishes of the family Myctophidae (Osteichthyes, Myctophiformes) from the 1979–Sargasso Sea expedition of R.V. Anton Dohrn. Annls. S. Afr. Mus. 96:19–53.

Infante, J. L. Z., and C. L. Cahu. 2001. Ontogeny of the gastrointestinal tract of marine fish larvae. Comp. Biochem. Physiol. C Toxicol. Pharmacol. 130:477–487.

Klingenberg, C. P. 2008. Morphological integration and developmental modularity. Annu. Rev. Ecol. Evol. Syst. 39:115–132.

———. 2009. Morphometric integration and modularity in configurations of landmarks: tools for evaluating a priori hypotheses. Evol. Dev. 11:405–421.

———. 2013. Cranial integration and modularity: insights into evolution and development from morphometric data. Hystrix 24:43–58.

———. 2014. Studying morphological integration and modularity at multiple levels: concepts and analysis. Philos. Trans. R. Soc. Lond. B Biol. Sci. 3691649:20130249, 9 pages.

Klingenberg, C. P., and J. Marugán-Lobón. 2013. Evolutionary covariation in geometric morphometric data: analyzing integration, modularity and allometry in a phylogenetic context. Syst. Biol. 62:591–610.

Klingenberg, C. P., K. Mebus, and J. C. Auffray. 2003. Developmental integration in a complex morphological structure: how distinct are the modules in the mouse mandible? Evol. Dev. 5:522–531.

Lanfear, R., B. Calcott, S. Y. W. Ho, and S. Guindon. 2012. PartitionFinder: combined selection of partitioning schemes and substitution models for phylogenetic analyses. Mol. Biol. Evol. 29:1695–1701.

Lauder, G. V., and E. D. Tytell. 2005. Hydrodynamics of undulatory propulsion. Fish Physiol. 23:425–468.

Lawry, J. V. Jr. 1973. Dioptric modifications of the scales overlying the photophores of the lantern fish, *Tarletonbeania crenularis* (Myctophidae). J. Anat. 114:55–63.

———. 1974. Lantern fish compare downwelling light and biouminescence. Nature 247:155–157.

Leroi, A. M. 2000. The scale independence of evolution. Evol. Dev. 2:67–77.

Loeb, V. J., A. K. Kellermann, P. Koubbi, A. W. North, and M. G. White. 1993. Antarctic larval fish assemblages: a review. Bull. Mar. Sci. 53:416–449.

Magwene, P. M. 2001. New tools for studying integration and modularity. Evolution 55:1734–1745.

Mahler, D. L., L. J. Revell, R. E. Glor, and J. B. Losos. 2010. Ecological opportunity and the rate of morphological evolution in the diversification of Greater Antillean anoles. Evolution 64:2731–2745.

Márquez, E. J. 2008. A statistical framework for testing modularity in multidimensional data. Evolution 62:2688–2708.

McGinnis, R. F. 1982. Biogeography of lanternfishes (Myctophidae) South of 30∘S. *In* D. L. Pawson, ed. Biology of the Antarctic Seas XII. American Geophysical Union, Washington, D.C, 110 pages.

Mitteroecker, P., and P. Gunz. 2009. Advances in geometric morphometrics. Evol. Biol. 36:235–247.

Monteiro, L. R., V. Bonato, and S. F. Dos Reis. 2005. Evolutionary integration and morphological diversification in complex morphological structures: mandible shape divergence in spiny rats (Rodentia, Echimyidae). Evol. Dev. 7:429–439.

Moser, H. G., and E. H. Ahlstrom. 1970. Development of lanternfishes (family Myctophidae) in the California Current. Part I. Species with narrow-eyed larvae. Bull. Los Angel. Cty. Mus. Nat. Hist. (Sci.) 7:1–145.

———. 1974. Role of larval stages in systematics investigations of marine teleosts: the Myctophidae, a case study. Fish. Bull. 72:391–413.

Moser, H. G., E. H. Ahlstrom, and J. R. Paxton. 1984. Myctophidae: development. Pp. 218–239 *in* H. G. Moser, W. J. Richard, D. M. Cohen, M. P. Fahay, A. W. Kendall Jr., and S. L. Richardson, eds. Ontogeny and systematics of fishes. American Society of Ichthyologists and Herpetologists, La Jolla, CA.

Near, T. J., A. Dornburg, M. Tokita, D. Suzuki, M. C. Brandley, and M. Friedman. 2014. Boom and bust: ancient and recent diversification in bichirs (Polypteridae: Actinopterygii), a relictual lineage of ray-finned fishes. Evolution 68:1014–1026.

Nosil, P. 2012. Ecological speciation. Oxford Univ. Press, Oxford, U.K.

O'Meara, B. C., C. Ané, M. J. Sanderson, and P. C. Wainwright. 2006. Testing for different rates of continuous trait evolution using likelihood. Evolution 60:922–933.

Olson, E. C., and R. L. Miller. 1958. Morphological integration. University of Chicago Press, Chicago, IL.

Osse, J. W. M. 1989. Form changes in fish larvae in relation to changing demands of function. Neth. J. Zool. 40:362–385.

Pakhomov, E. A., R. Perissinotto, and C. D. McQuaid. 1996. Prey composition and daily rations of myctophid fishes in the Southern Ocean. Mar. Ecol. Prog. Ser. 134:1–14.

Paxton, J. R. 1972. Osteology and relationships of the lanternfishes (family Myctophidae). Bull. Nat. Hist. Mus. Los Angel. Cty. Sci. 13:1–81.

Pietsch, T., and J. Orr. 2007. Phylogenetic relationships of deep-sea anglerfishes of the suborder Ceratioidei (Teleostei: Lophiiformes) based on morphology. Copeia 2007:1–34.

Poulsen, J. Y., I. Byrkjedal, E. Willassen, D. Rees, H. Takeshima, T. P. Satoh, G. Shinohara, M. Nishida, and M. Miya. 2013. Mitogenomic sequences and evidence from unique gene rearrangements corroborate evolutionary relationships of Myctophiformes (Neoteleostei). BMC Evol. Biol. 13:111.

Price, S. A., P. C. Wainwright, D. R. Bellwood, E. Kazancioglu, D. C. Collar, and T. J. Near. 2010. Functional innovations and morphological diversification in parrotfish. Evolution 64:3057–3068.

Price, S. A., R. Holzman, T. J. Near, and P. C. Wainwright. 2011. Coral reefs promote the evolution of morphological diversity and ecological novelty in labrid fishes. Ecol. Lett. 14:462–469.

Price, S. A., J. J. Tavera, T. J. Near, and P. C. Wainwright. 2013. Elevated rates of morphological and functional diversification in reef-dwelling haemulid fishes. Evolution 67:417–428.

Rabosky, D. L. 2014. Automatic detection of key innovations, rate shifts, and diversity-dependence on phylogenetic trees. PLoS One 9:e89543.

Ray, D. L. 1950. The peripheral nervous system of *Lampanyctus leucopsaurus*. J. Morphol. 87:61–178.

Revell, L. J. 2013. Ancestral character estimation under the threshold model from quantitative genetics. Evolution 68:743–759. dx10.1111/evo.12300.

Rohlf, F. J. 2010. TPSDig2 version 2.16. Department of Ecology and Evolution, Stony Brook, NY.

Rohlf, F. J., and M. Corti. 2000. The use of two-block partial least-squares to study covariation in shape. Syst. Biol. 49:740–753.

Rohlf, F. J., and D. E. Slice. 1990. Extensions of the Procrustes method for the optimal superimposition of landmarks. Syst. Zool. 39:40–59.

Sabatés, A., and E. Saiz. 2000. Intra-and interspecific variability in prey size and niche breadth of myctophiform fish larvae. Mar. Ecol. Prog. Ser. 201:261–271.

Sanger, T. J., D. L. Mahler, A. Abzhanov, and J. B. Losos. 2012. Roles for modularity and constraint in the evolution of cranial diversity among *Anolis* lizards. Evolution 66:1525–1542.

Sassa, C., K. Kawaguchi, Y. Hirota, and M. Ishida. 2007. Distribution depth of the transforming stage larvae of myctophid fishes in the subtropical–tropical waters of the western North Pacific. Deep Sea Res. Part I Oceanogr. Res. Pap. 54:2181–2193.

Sauvage, H. E. 1873. Memoire sur la faune ichthyologique de la période tertiare et plus spécialment sur les poissons fossiles d'Oran (Algérie) et sur ceux découveris par M.R. Alby a Licata en Sicile. Annales des Sciences Géologiques 4:1–272.

Schwarz, G. E. 1978. Estimating the dimension of a model. Ann. Stat. 6:461–464.

Sidlauskas, B. 2008. Continuous and arrested morphological diversification in sister clades of characiform fishes: a phylomorphospace approach. Evolution 62:3135–3156.

Simpson, G. G. 1944. Tempo and mode in evolution. Columbia Univ. Press, New York, NY.

Smilde, A. K., H. A. L. Kiers, S. Bijlsma, C. M. Rubingh, and M. J. VanErk. 2009. Matrix correlations for high-dimensional data: the modified RV-coefficient. Bioinformatics 25:401–405.

Team, R. D. C. 2014. R: a language and environment for statistical computing. R Foundation for Statistical Computing, Vienna, Austria.

Tsarin, S. A. 1999. Character of aggregation of myctophids in the tropical zone of the Indian Ocean. Hydrobiol. J. 35:59–67.

Turner, J. R., E. M. White, M. A. Collins, J. C. Partridge, and R. H. Douglas. 2009. Vision in lanternfish (Myctophidae): adaptations for viewing bioluminescence in the deep-sea. Deep Sea Res. Part I Oceanogr. Res. Pap. 56:1003–1017.

Van Valen, L. M. 1971. Adaptive zones and the orders of mammals. Evolution 25:420–428.

Wagner, C. E., L. J. Harmon, and O. Seehausen. 2012. Ecological opportunity and sexual selection together predict adaptive radiation. Nature 487:366–369.

Wagner, G. P. 1996. Homologues, natural kinds and the evolution of modularity. Am. Zool. 36:36–43.

Wagner, G. P., and L. Altenberg. 1996. Perspective: complex adaptations and the evolution of evolvability. Evolution 50:967–976.

Wagner, G. P., M. Pavlicev, and J. M. Cheverud. 2007. The road to modularity. Nat. Rev. Genet. 8:921–931.

Webb, P. W. 1984. Body form, locomotion and foraging in aquatic vertebrates. Am. Zool. 24:107–120.

Weihs, D. 1974. Energetic advantages of burst swimming of fish. J. Theor. Biol. 48:215–229.

Widder, E. A. 2010. Bioluminescence in the ocean: origins of biological, chemical, and ecological diversity. Science 328:704–708.

Associate Editor: J. Tobias
Handling Editor: J. Conner

Supporting Information

Additional Supporting Information may be found in the online version of this article at the publisher's website:

Figure S1. Statistical power curves for tests comparing evolutionary rates for two groups of taxa on random phylogenies.
Figure S2. Estimation of magnitude of difference in inferred high-dimensional evolutionary rates when landmarks are assigned to incorrect modules, under varying simulation conditions.
Figure S3. (A) Histogram of rate ratios for 1000 simulated datasets, comparing evolutionary rates for shapes based on eight landmarks to those based on four landmarks.
Table S1. Type I error results at increasing levels of trait covariation.